Modeling crawling cell movement

J. Löber[1] F. Ziebert[2] I. S. Aranson[3]

[1]Institute of Theoretical Physics
TU Berlin

[2]Institute of Physics
University of Freiburg

[3]Materials Science Division
Argonne National Laboratory

Group Seminar, April 2014

Introduction

- several moving cells[1]
- Top left: mouse fibroblasts moving into an artificial wound (total video time: 3h)
- Bottom left: chick fibroblasts (total video time: 2h)
- Top right: mouse melanoma cell (total video time: 20min)
- Bottom right: trout epidermal keratocyte (total video time: 4min)

[1] Video from: A Video Tour of Cell Motility, http://cellix.imba.oeaw.ac.at/

Sketch of cell cross section

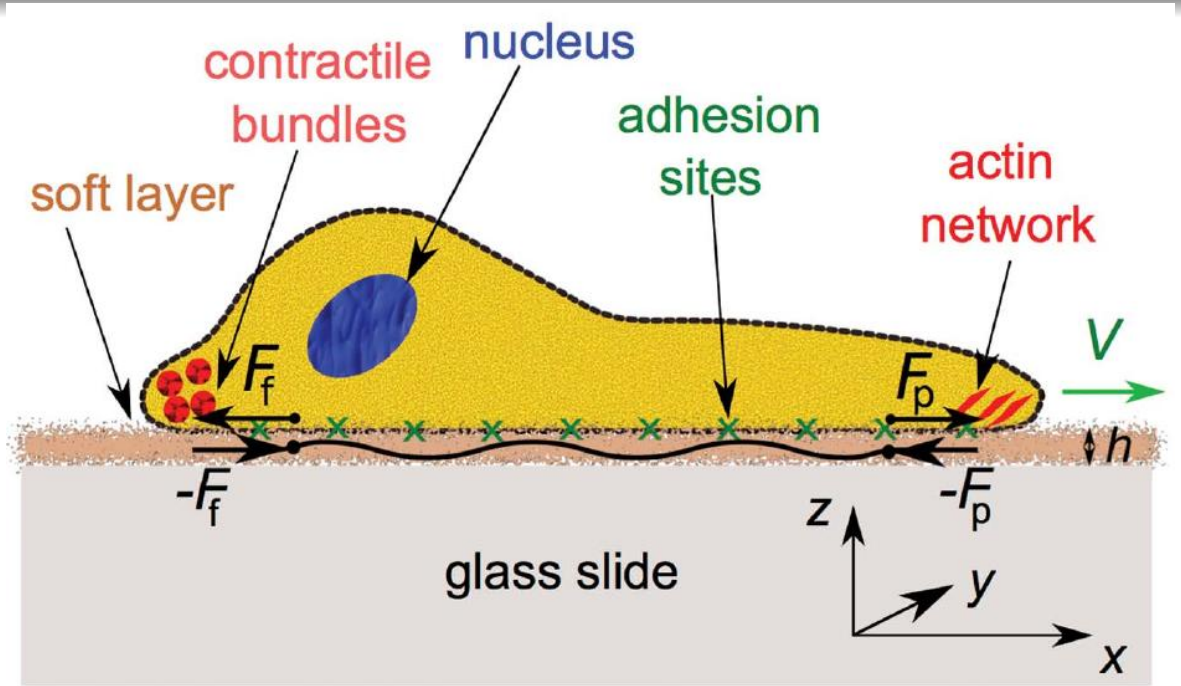

[2]

- 2D cell shape modeled by phase field $\rho(x, y, t)$
- $\rho = 1$: cell, $\rho = 0$: no cell
- we neglect variations in height of cell
- nucleus rolls behind the lamellipodium front[3]

[2] Image from: F. Ziebert and I. S. Aranson, PLOS ONE, **8**, e64511.
[3] Video from: A Video Tour of Cell Motility, http://cellix.imba.oeaw.ac.at/

Actin cytoskeleton

- cell crawling is driven by the continuous reorganization and turnover of the actin cytoskeleton
- two functions
  - protrusion by polymerization
  - contraction by interaction with myosin
- modeled by average actin orientation field $\mathbf{p} = \begin{pmatrix} p_x(x,y,t) \\ p_y(x,y,t) \end{pmatrix}$[4]

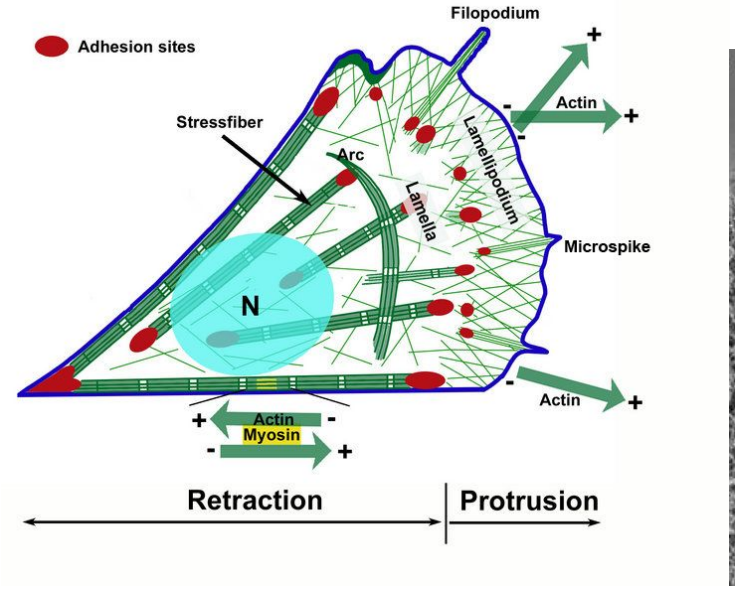

(a) Schematics of actin network

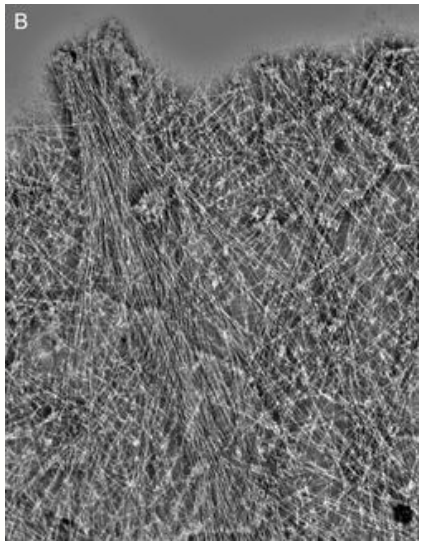

(b) Closeup of actin filaments

[4] Images from: A Video Tour of Cell Motility, http://cellix.imba.oeaw.ac.at/

Adhesion sites

- adhesion sites connect the actin network to the substrate
- video: adhesion sites (red)[5]
- modeled by concentration of adhesion sites $A(x, y, t)$
- adhesion sites do not move with the cell
- rupture of adhesion sites in the retracting region of the cell

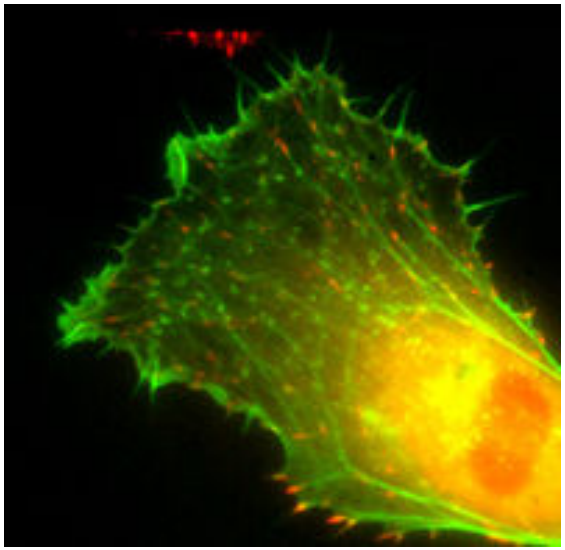

[5] JV Small, B Geiger, I. Kaverina, A. Bershadsky, Nat. Rev. Mol. Cell Biol. **3**, 957 (2002).

Myosin

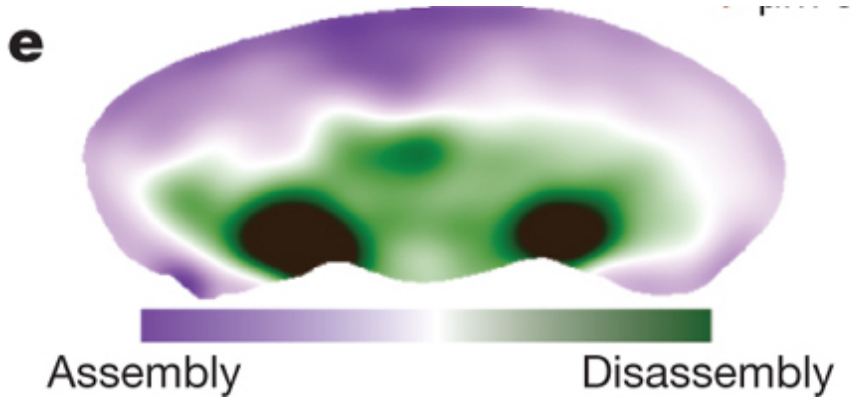

(c) Sites of actin assembly and disassembly

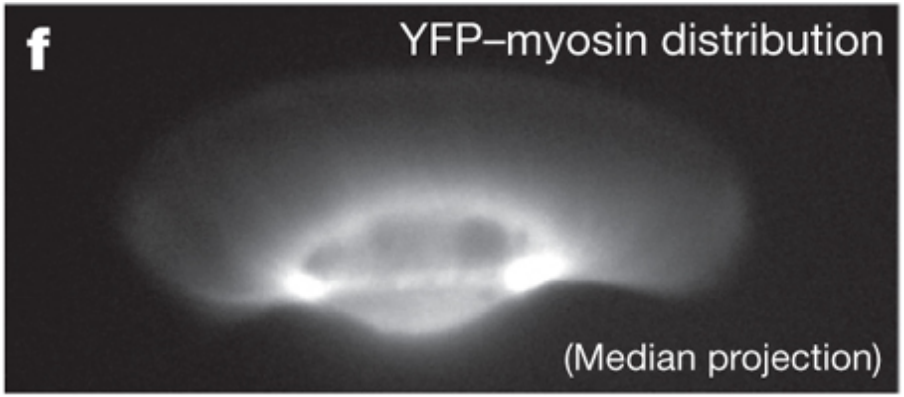

(d) Concentration of myosin

- myosin concentration is high where actin is disassembled[6]
- could be modeled by an extra field $m(x, y, t)$ but is eliminated in our model

[6] CA Wilson et al. Nature **465**, 373 (2010).

Traction and substrate displacements

- cell exerts traction forces $\mathbf{T} = \begin{pmatrix} T_x(x,y,t) \\ T_y(x,y,t) \end{pmatrix}$ on substrate
- leads to substrate displacements[7]: $\mathbf{u} = \begin{pmatrix} u_x(x,y,t) \\ u_y(x,y,t) \end{pmatrix}$

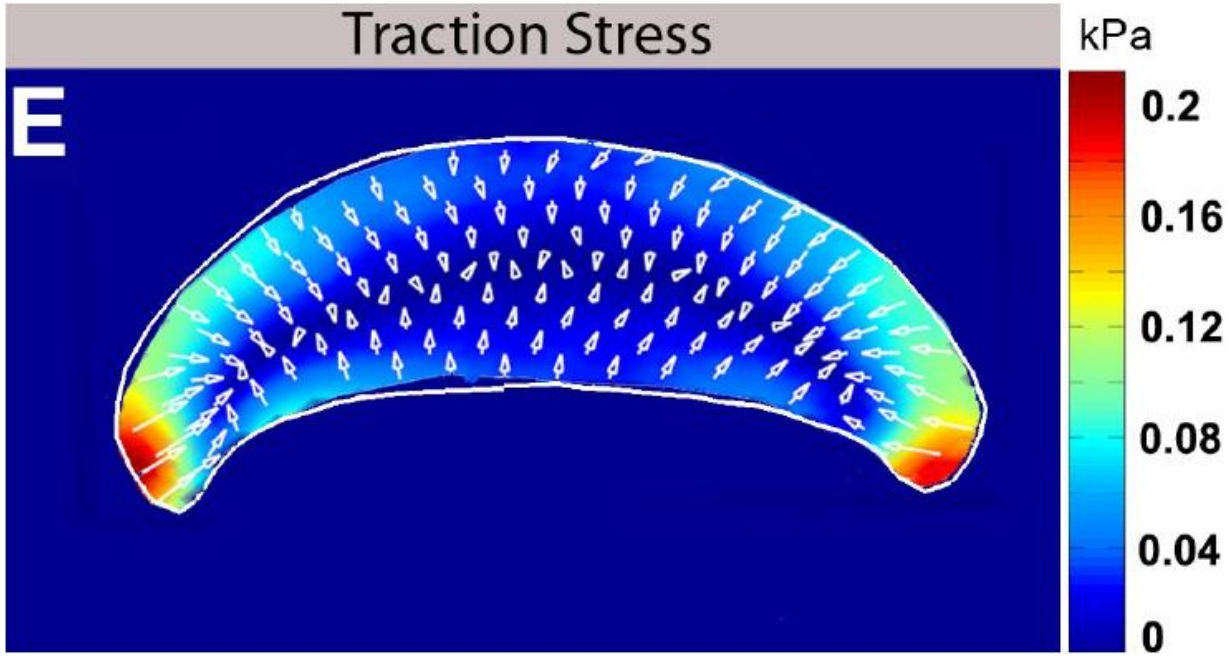

[7] MF Fournier, R Sauser, D Ambrosi, JJ Meister, AB Verkhovsky, J. Cell Biol. **188**, 287 (2010).

Phase field $\rho(x,y,t)$

- phase field: $\rho = 1$: cell, $\rho = 0$: no cell, $\nabla\rho \neq 0$: cell boundary

$$\partial_t \rho = D_\rho \Delta\rho - (1-\rho)(\delta-\rho)\rho - \alpha A \mathbf{p} \cdot (\nabla\rho)$$

- $\rho(x) = 1/\left(1+\exp\left(x/\sqrt{D_\rho 2}\right)\right)$ is a steplike stationary solution for $\delta = 1/2$: Mathematica
- volume conservation by feedback
  - $\langle\rho\rangle$ =volume integral over ρ
  - V_0: initial volume
  - $\sigma|\mathbf{p}|^2$ models actin network contraction

$$\delta = \frac{1}{2} + \mu(\langle\rho\rangle - V_0) - \sigma|\mathbf{p}|^2$$

- advection of ρ along the actin orientation vector $\mathbf{p}$, α: propulsion strength

Actin orientation field $\mathbf{p}(x, y, t)$

$$\partial_t \mathbf{p} = D_p \Delta \mathbf{p} - \tau_1^{-1} \mathbf{p} - \tau_2^{-1} \left(1 - \rho^2\right) \mathbf{p} - \beta f(\nabla \rho) - \gamma \left[(\nabla \rho) \cdot \mathbf{p}\right] \mathbf{p}$$

- nearest neighbour interaction by diffusion D_p
- degradation of actin by depolymerization inside (τ_1) and outside (τ_2) of the cell
- actin created by polymerization at the cell front, $f(\kappa) = \frac{\kappa}{\sqrt{1+\epsilon\kappa^2}}$ saturates for large κ
- reflection symmetry broken due to myosin motors

Myosin concentration $m(x,y,t)$

- actin disassembles where myosin concentration is higher than equilibirum value m_0

$$\partial_t \mathbf{p} = D_p \Delta \mathbf{p} - \tau_1^{-1} \mathbf{p} - \tau_2^{-1} \left(1 - \rho^2\right) \mathbf{p} - \beta f(\nabla \rho) - (m - m_0) \mathbf{p}$$

- myosin
  - diffuses with coefficient D_m
  - relaxes to m_0 with rate τ_m
  - moves along the actin filaments with velocity V_m
  - is supressed near to front of the cell with rate $\bar{\gamma} \nabla \rho \cdot \mathbf{p}$

$$\partial_t m = D_m \Delta m - \tau_m^{-1} (m - m_0) + V_m \mathbf{p} \cdot \nabla m + \bar{\gamma} \nabla \rho \cdot \mathbf{p}$$

- assume $\tau_m \ll 1$

$$m - m_0 \approx \tau_m \bar{\gamma} \nabla \rho \cdot \mathbf{p}$$

Concentration of adhesion sites $A(x, y, t)$

$$\partial_t A = D_A \Delta A + a_0 \rho p^2 + a_{nl} \rho A^2 - s A^3 - d(|\mathbf{u}|) A$$

- adhesion sites form only if actin is present but independent of actin direction: linear attachment $\sim \rho p^2$
- already formed adhesion complex favors formation of more adhesive contacts nearby: nonlinear attachment $\sim A^2$
- nonlinear detachment $\sim A^3$ locally saturates concentration of adhesion sites
- breakup of adhesion sites if substrate displacement $|\mathbf{u}|$ exceeds critical displacement U_c: linear step-like detachment rate

$$d(|\mathbf{u}|) = \frac{d}{2}\left(1 + \tanh\left[b\left(\mathbf{u}^2 - U_c^2\right)\right]\right)$$

Substrate model: Kelvin-Voigt material

- stress tensor of 3D incompressible isotropic visco-elastic (Kelvin-Voigt) material
  $\mathbf{u}$: displacements, p: pressure, $\tilde{G}$: shear modulus, $\tilde{\eta}$: viscosity

$$\sigma_{ik} = \tilde{G}\left(u_{i,k} + u_{k,i}\right) + \tilde{\eta}\left(\dot{u}_{i,k} + \dot{u}_{k,i}\right) - p\delta_{ik}$$

- overdamped motion: $\ddot{u}_i = 0$, $\sigma_{ik,k} = 0$

$$\tilde{G}\nabla^2\mathbf{u} + \tilde{\eta}\nabla^2\dot{\mathbf{u}} = \nabla p, \qquad \nabla\cdot\mathbf{u} = 0$$

- lower boundary conditions: $\mathbf{u}\left(x, y, z = 0, t\right) = 0$
- upper boundary conditions: traction force $\mathbf{T}$, H: height of substrate layer

$$\begin{aligned}
\sigma_{xz}\left(x, y, z = H, t\right) &= T_x\left(x, y, t\right), \\
\sigma_{yz}\left(x, y, z = H, t\right) &= T_y\left(x, y, t\right), \\
\sigma_{zz}\left(x, y, z = H, t\right) &= 0,
\end{aligned}$$

- periodic boundary conditions in x-, y- direction with period L

Substrate model: traction forces $\mathbf{T}(x, y, t)$

- integrate over z- direction
- assume height $\ll$ lateral extension: $H \ll L$, expand in H/L

$$\partial_t \mathbf{u} = -\frac{1}{\eta}\left(G\mathbf{u} - \frac{1}{\xi}\left(\mathbf{T} + h\left[5\Delta\mathbf{T} + 19\nabla\left(\nabla\cdot\mathbf{T}\right)\right]\right)\right)$$

- traction due to actin polymerization: $\mathbf{T}_{\mathrm{pr}} = -\xi\rho A\mathbf{p}$
- traction due to friction: $\mathbf{T}_{\mathrm{fr}} = \rho A\boldsymbol{\zeta}$
- cell does not exert a net force on substrate: determine $\boldsymbol{\zeta}$ by $\left\langle \mathbf{T}_{\mathrm{pr}} + \mathbf{T}_{\mathrm{fr}} \right\rangle = 0$

$$\mathbf{T} = \xi A\rho\frac{\langle A\mathbf{p}\rho\rangle}{\langle A\rho\rangle} - \xi A\rho\mathbf{p}$$

- for heterogeneous substrate, shear modulus G (stiffness) depends on space

Cell shape

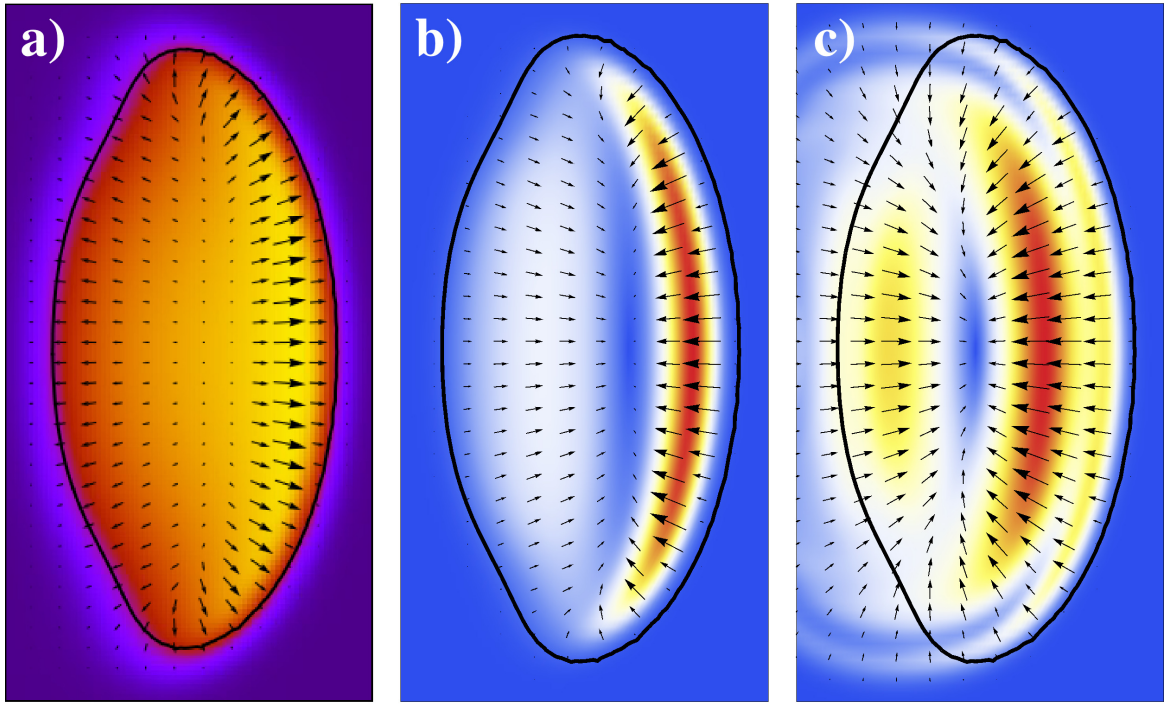

Figure: Shape of cells in the steady moving regime. Black contour: $\rho = 0.25$. a) Actin orientation field **p**. b) Traction force **T**. Red (blue) corresponds to large (small) values of |**T**|. c) Displacements field **u**. Red (blue) corresponds to large (small) values of |**u**|.

Phase diagram

Propulsion strength α vs. substrate's shear modulus G

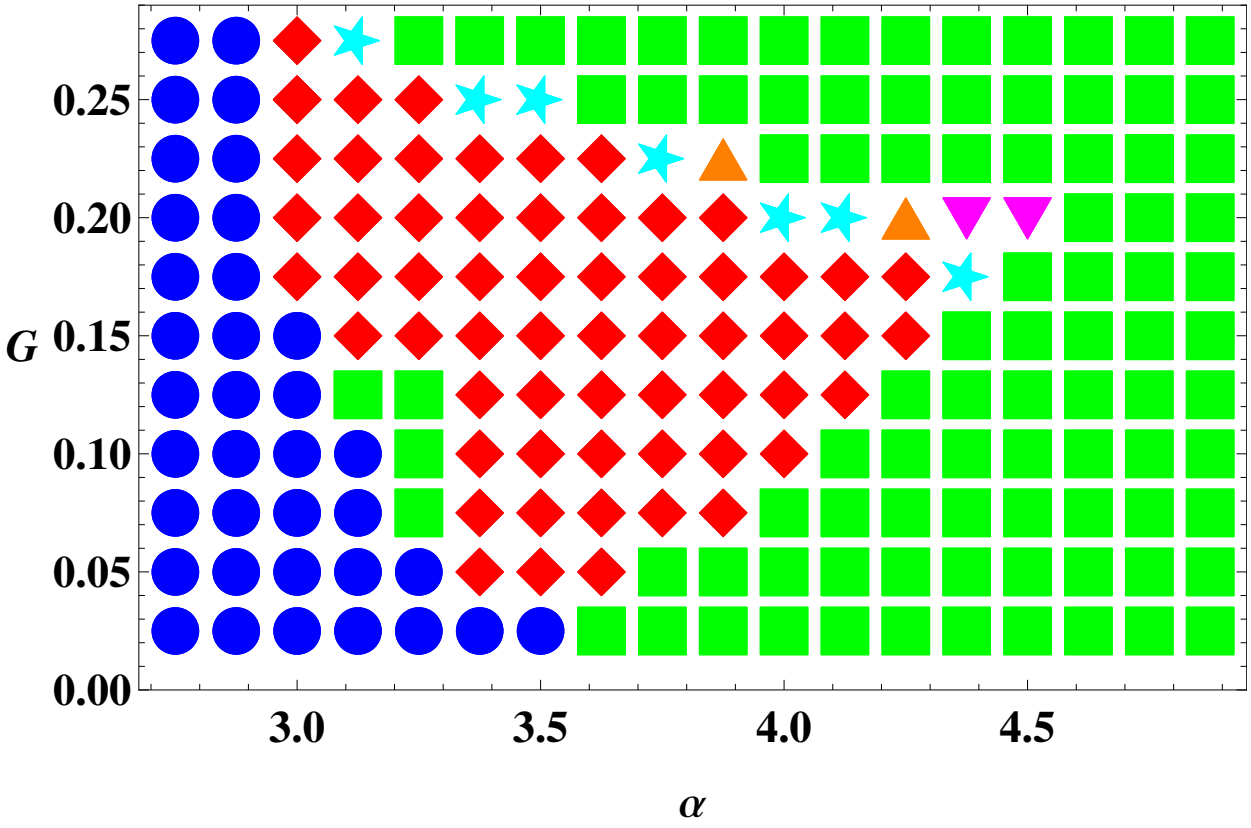

Figure: Phase diagram for propulsion strength α vs. substrate's shear modulus G. ● denotes non-moving states, ■ steady moving (gliding) states, ◆ stick-slip motion, ★ wandering bipedal and ▼, ▲ breathing and bipedal modes, respectively.

Stick-slip motion

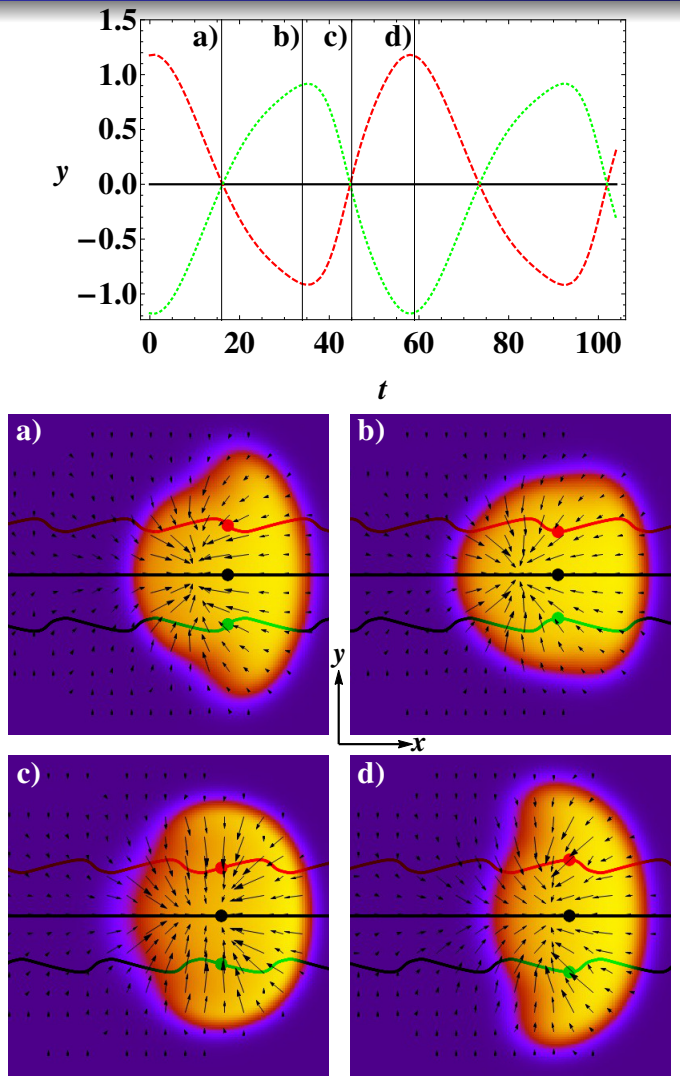

Figure: Cell shape and substrate displacement field.

- top panel: y-component of center of mass (c.o.m.) of upper (red) and lower (green) half of cell
- x-component does not show oscillations
- overall c.o.m. (black line) moves in a straight line
- compare with experiment[a]

[a] K. Keren et al. Nature **453**, 475 (2008).

Bipedal motion

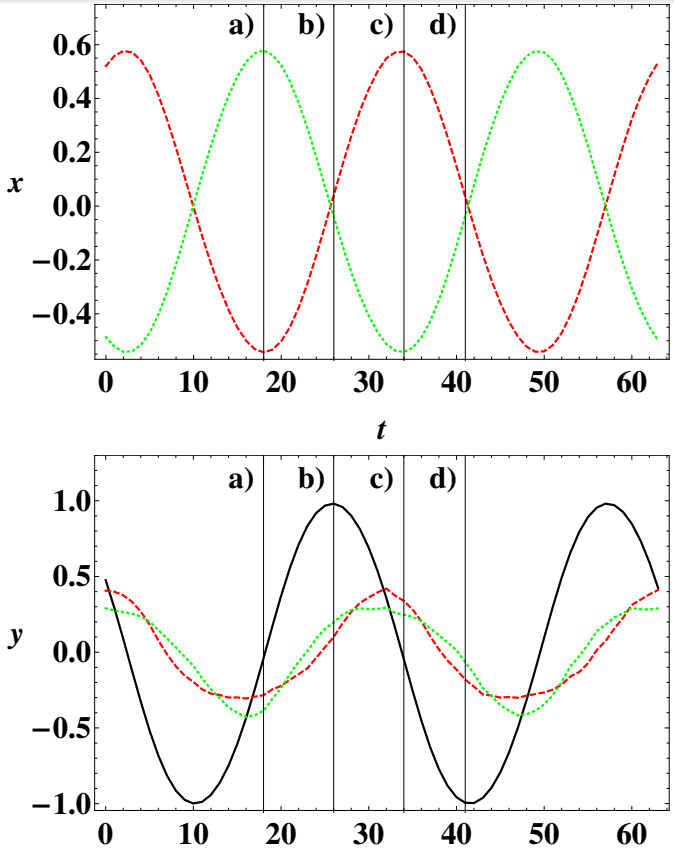

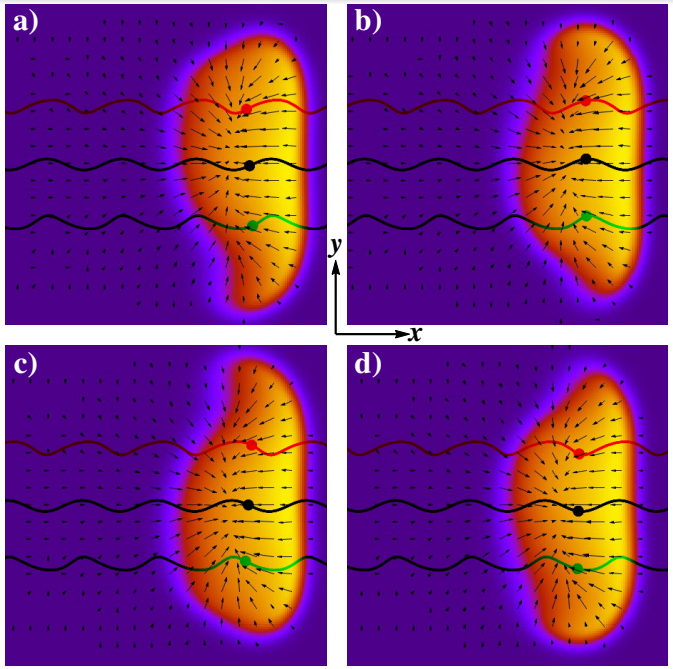

- anti-phase oscillations of c.o.m. x- components of upper (red) and lower (green) cell half
- in-phase oscillations of y- components
- c.o.m. (black) also oscillates compare with experiment 1[8] 2

[8] EL Barnhart, GM Allen, F Jülicher, JA Theriot, Biophys. J. **98**, 933 (2010).

Wandering bipedal

- instability in the propagation direction
- similar behavior found in a simple model for deformable self-propelled particles [9]:
  - drift bifurcation leads from stationary to moving states
  - 2nd bifurcation leads from straight motion to circular motion

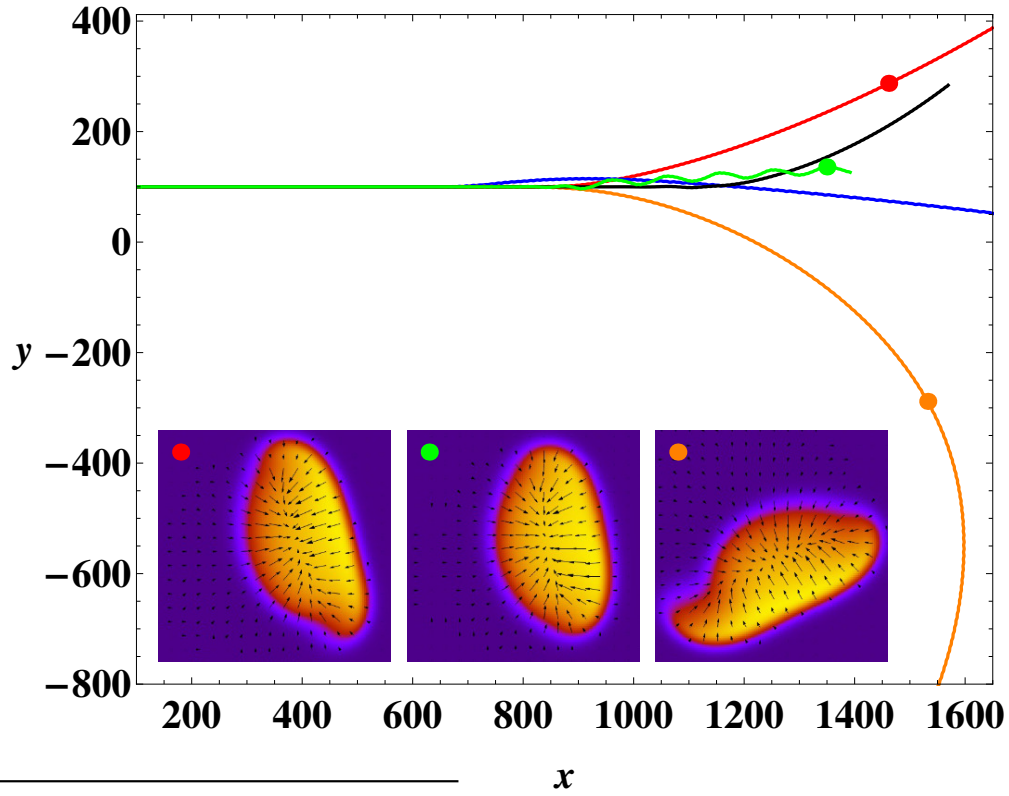

[9] T. Ohta, T. Ohkuma, PRL **102**, 154101 (2009).

Durotaxis (cell migration in a stiffness gradient)

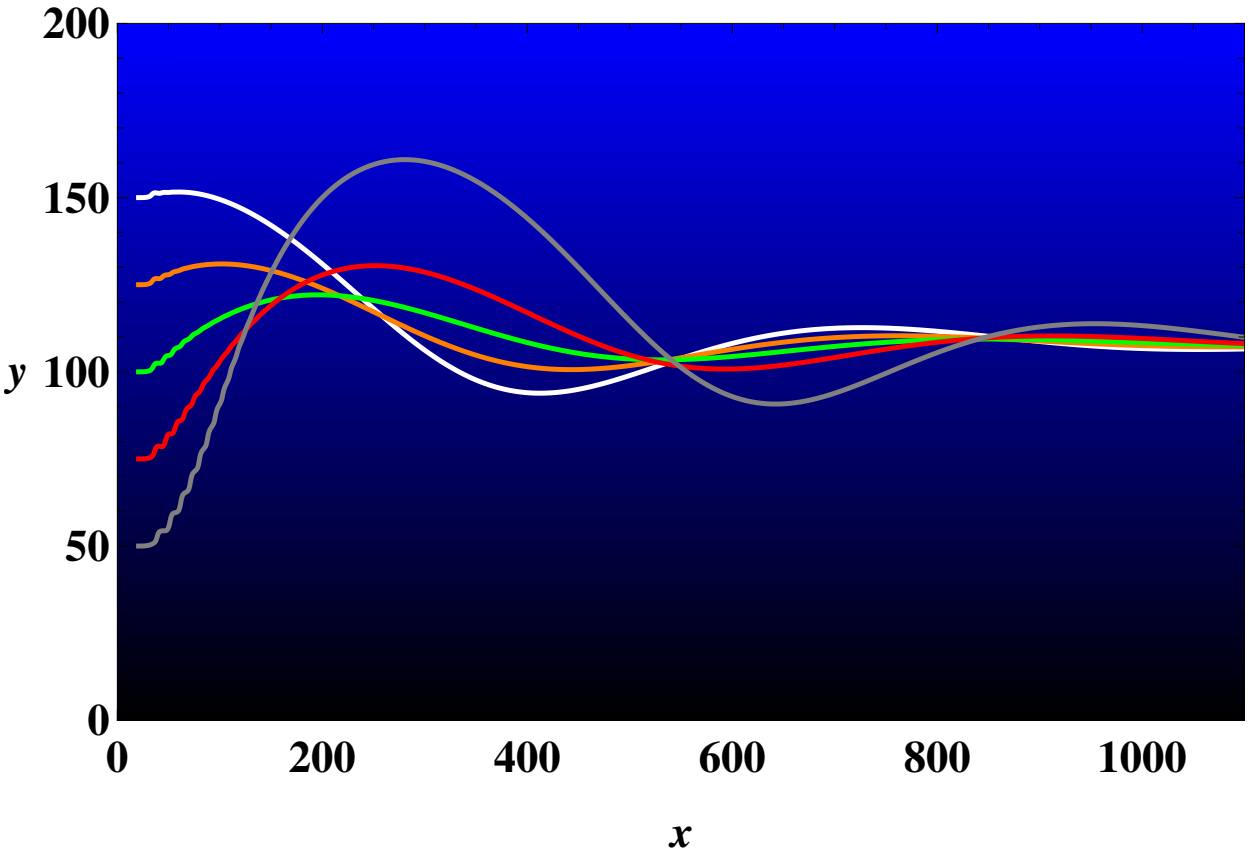

Figure: A linear gradient in substrate's stiffness G in the y-direction from $G = 0$ (black) at the bottom to $G = 0.4$ (blue) at the top. The curves show center of mass trajectories for different initial positions. They converge to an optimal value of G.

Stiffness step

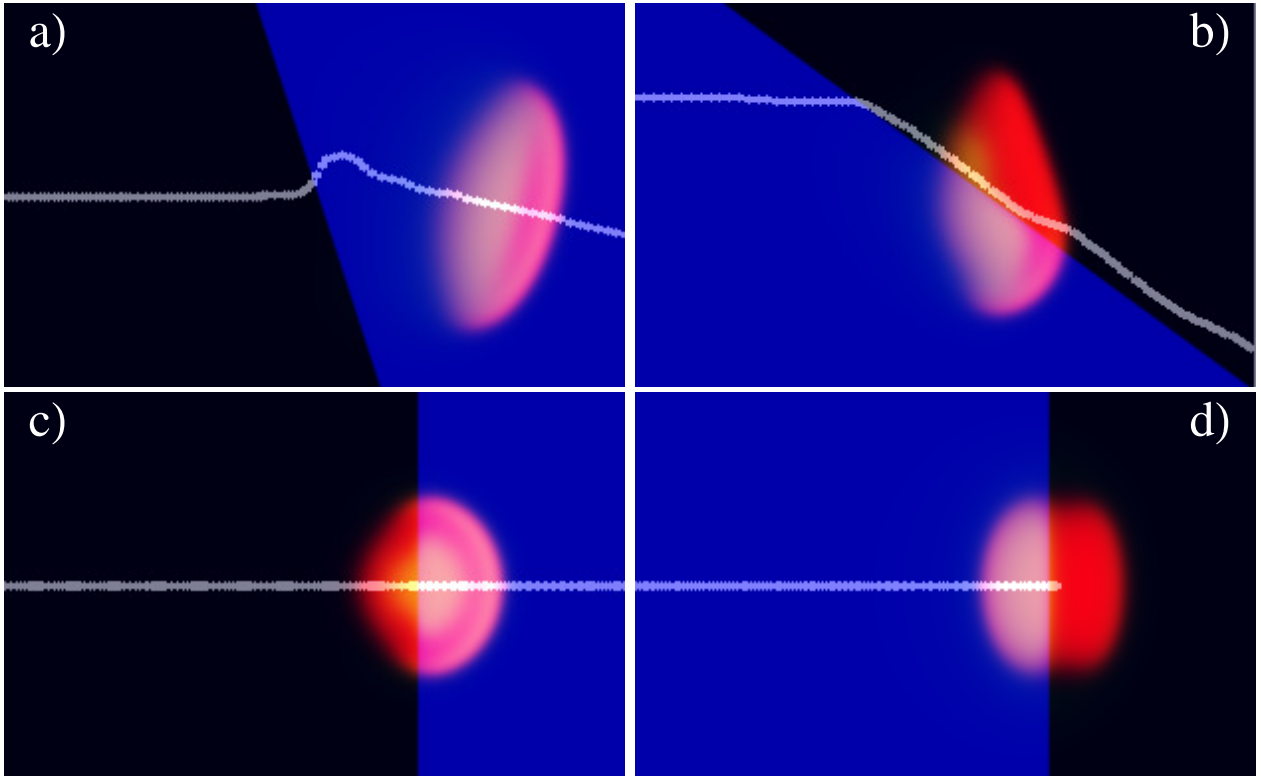

Figure: Examples for the behavior of cells colliding with a step in the substrate stiffness (blue: $G = 0.4$, black: $G = 0.05$). The center of mass trajectories are shown in white. Top row: $\alpha = 4 = 2\beta$, bottom row: $\alpha = 4, \beta = 1.5$. Other parameters: $U_c^2 = 0.25$.

Cell-cell interaction with mutiple phase fields

- phase fields ρ_i for N cells

$$\partial_t \rho_i + \alpha A \mathbf{p} \cdot \nabla \rho_i = D_\rho \triangle \rho_i - \frac{\partial}{\partial \rho_i} V(\rho_i) - \frac{\partial}{\partial \rho_i} W(\rho_1, \ldots, \rho_N), \; i = 1, \ldots, N.$$

- V : self-interaction $\quad \frac{\partial}{\partial \rho_i} V(\rho_i) = \rho_i (\rho_i - \delta_i)(\rho_i - 1)$
- W : volume (steric) interaction avoids interpenetration of cells

$$W(\rho_1, \ldots, \rho_N) = \sum_{j,k} W_2(\rho_j, \rho_k)$$

- two cell pair potential $\quad W_2(\rho_1, \rho_2) = \frac{\lambda}{2} \rho_1^m \rho_2^n$
  - large and positive if the two cells overlap
  - zero for no overlap
  - W_2 does not depend on m, n in the sharp interface limit $D_\rho \to 0$
  - for $D_\rho > 0$ perturbations could lead to $\rho_i < 0 \Rightarrow$ choose even exponents $m = n = 2$ to avoid attraction
- all other fields are shared between cells. Video. Experiment.[10]

[10] http://cellix.imba.oeaw.ac.at/

Alignment mechanism responsible for collective motion

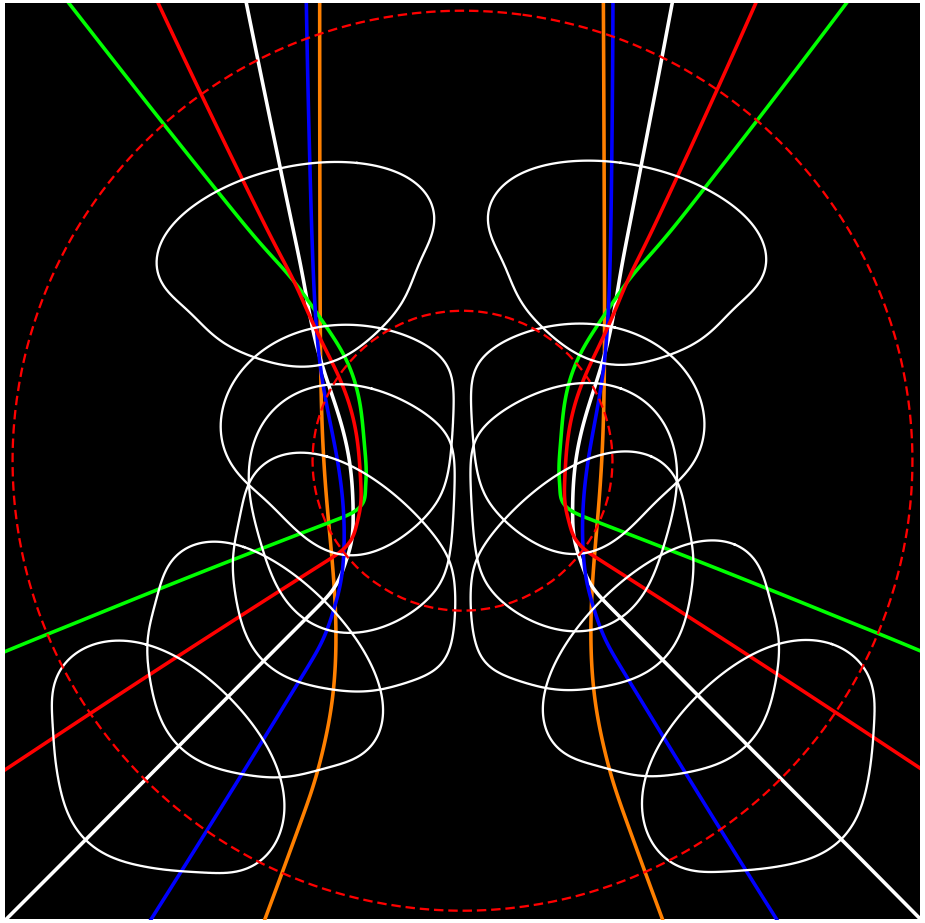

Figure: The angle of incidence of two cells colliding in a symmetric fashion is larger than their exit angles. White: phase field contours with $\rho = 0.5$. Colored: trajectories of colliding cell for different angles of incidence. See video.

Unidirectional collective motion

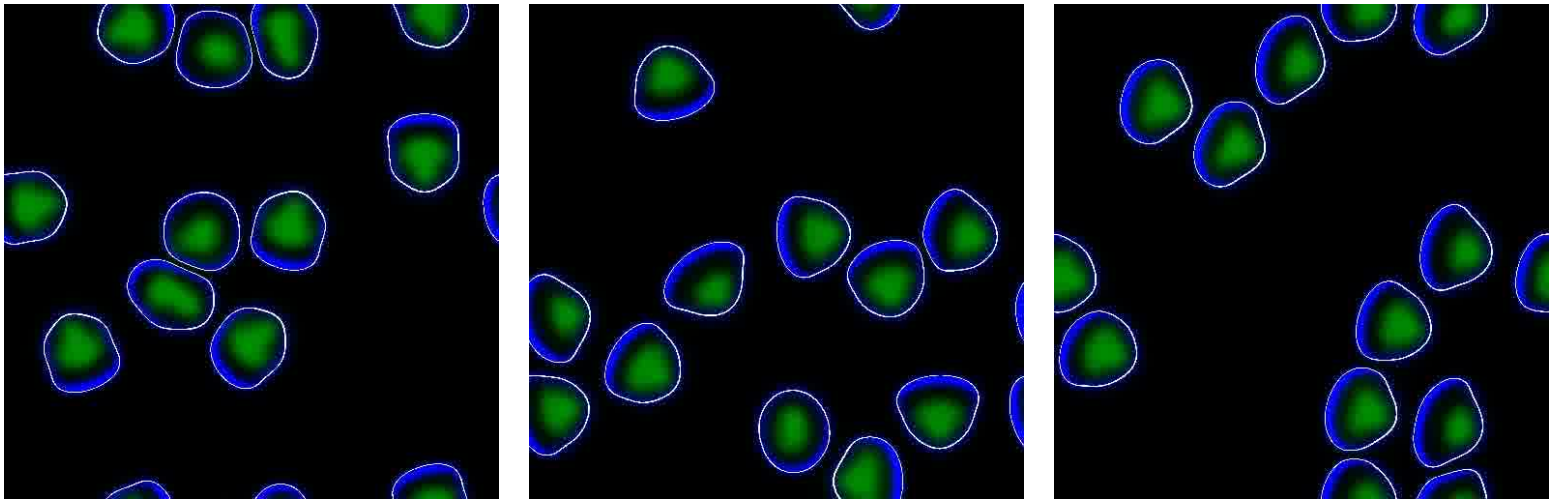

Figure: Initially, cells move uncorrelated. The alignment mechanism leads to an unidirectional collective motion towards the top left corner. Time is increasing from left to right. Video. Experiment from Phys. Rev. E **74**, 061908 (2006).

Coexistence of moving and stationary cells

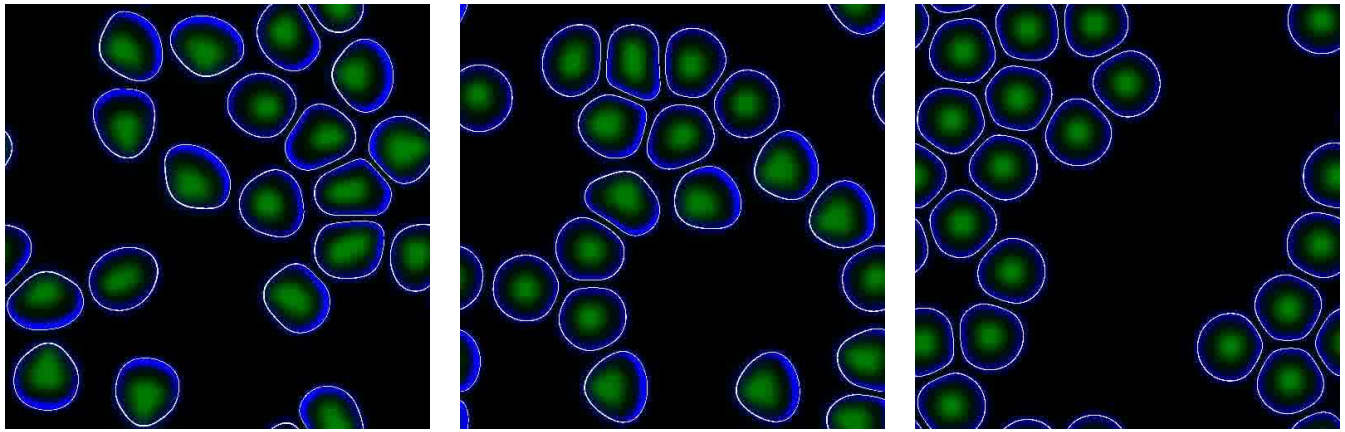

Figure: Initially moving cells gather in stationary clusters. See video.

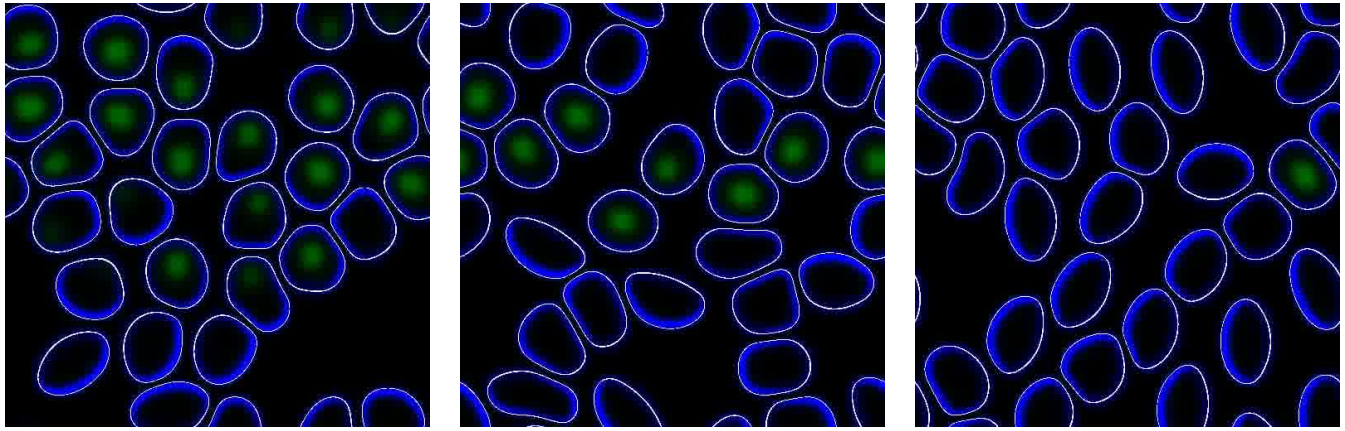

Figure: Initially, some cells are moving while some are stationary. Cell-cell collisions set the stationary cells into motion. See video.

Collective rotational motion

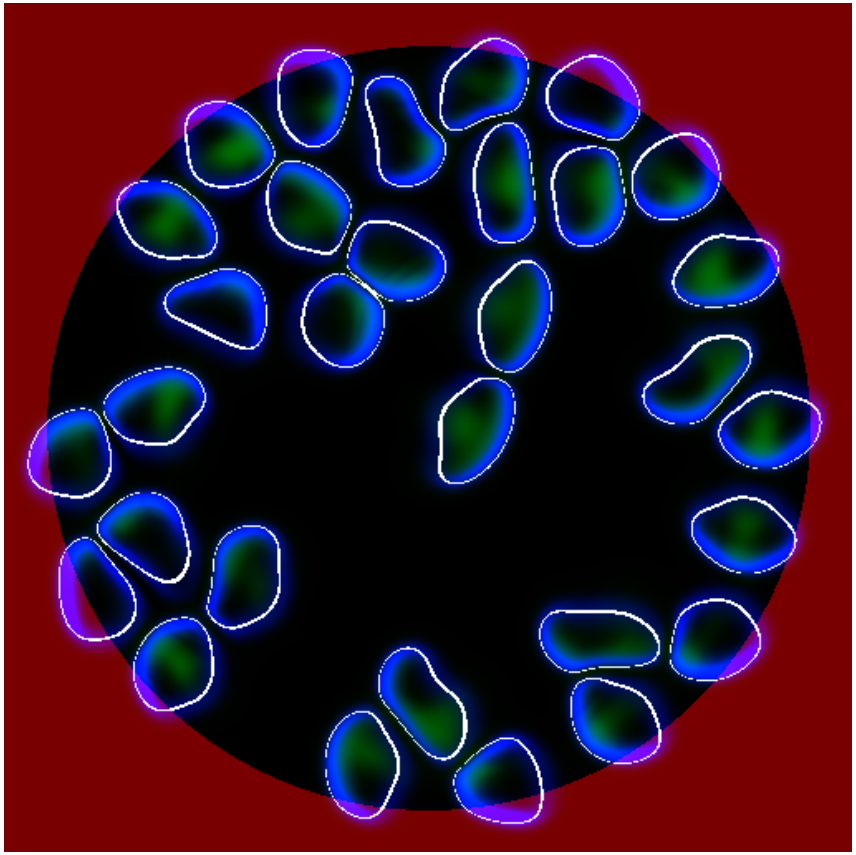

Figure: Clockwise rotational motion in a confined medium. Adhesion is larger inside. Video. Experiment (Phys. Rev. E **74**, 061908 (2006)).

order parameter ϕ

$$\phi(t) = \frac{1}{N}\sum_{i=1}^{N} \hat{\mathbf{e}}_\theta(t)\cdot\hat{\mathbf{v}}_i(t)$$

normalized velocity vector $\hat{\mathbf{v}}_i(t) = \frac{\mathbf{v}_i(t)}{|\mathbf{v}_i(t)|}$ for each cell i is projected onto the unit vector $\hat{\mathbf{e}}_\theta$ tangential to a circle

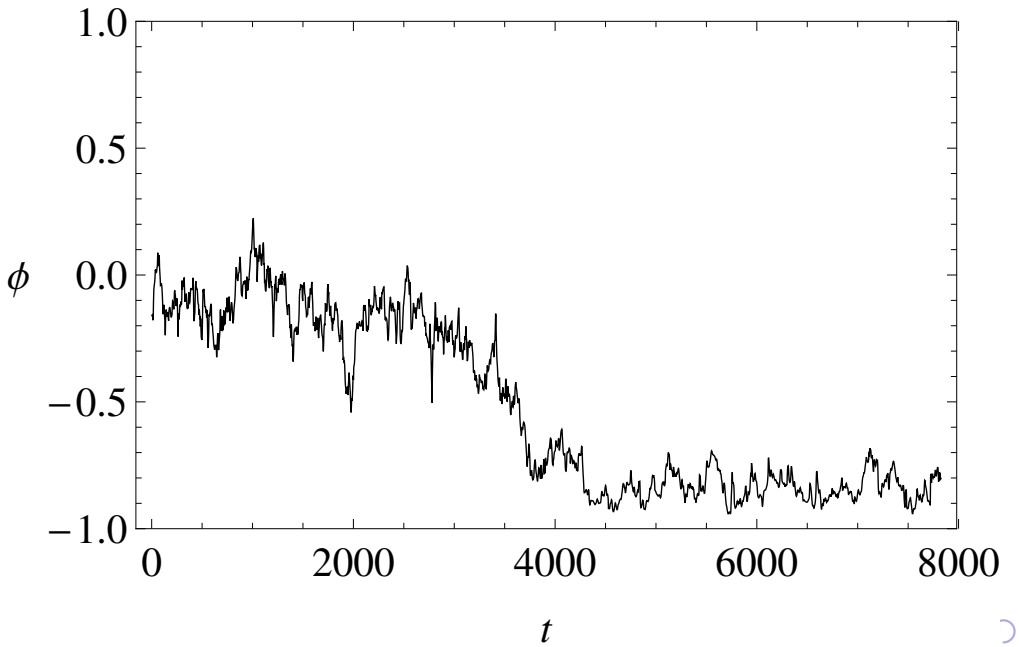

Adhesion between cells

- keratocytes are responsible for wound healing ⇒ can build cell monolayers
- cell boundaries located at $\nabla\rho_i$
- adhesion = interaction between cell boundaries: $\nabla\rho_i \cdot \sum_{j\neq i} \nabla\rho_j$

$$\partial_t \rho_i + \alpha A \mathbf{p} \cdot \nabla\rho_i + \kappa \underbrace{\nabla\rho_i \cdot \sum_{j\neq i} \nabla\rho_j}_{\text{cell-cell adhesion}} = D_\rho \triangle\rho_i - \frac{\partial}{\partial\rho_i} V(\rho_i) - \frac{\partial}{\partial\rho_i} W(\rho_1, \ldots, \rho_N)$$

- multiple cells with cell-cell adhesion
- increasing adhesion strength κ should yield a transition to tissue (= cells sticking firmly together) but gives numerical instabilities instead
- other possibilities:[11]

[11] Study on multicellular systems using a phase field model, M. Nonomura, PloS one **7**, e33501 (2012).

Summary

- phenomenological model for crawling cells based on a reaction-diffusion system
- cells exhibit different modes of movement accompanied by shape changes similar to experiments
  - stick-slip motion
  - bipedal motion
- migration of cells is sensitive to mechanical properties of substrate
- collective motion of multiple cells modeled with interacting phase fields

Outlook

- introduce different adhesion terms to model tissue
- fit model parameters to specific cell types
- avoid breakup of cells
- derive model equations in a more fundamental way as e.g. in [12]

[12] Generic theory of active polar gels: a paradigm for cytoskeletal dynamics, K. Kruse, J.F. Joanny, F. Jülicher, J. Prost, K. Sekimoto, Eur. Phys. J. E **16**, 5 (2005).

For Further Reading I

J. Löber, F. Ziebert, and I. S. Aranson.
Modeling crawling cell movement on soft engineered substrates.
Soft Matter **10**, 1365 (2014).

F. Ziebert, S. Swaminathan, and I. S. Aranson.
J. R. Soc. Interface **9**, 1084 (2012).

F. Ziebert, and I. S. Aranson.
PLOS ONE, **8**, e64511.

For Further Reading II

- B. A. Camley, Y. Zhao, B. Li, H. Levine, and W.-J. Rappel. Phys. Rev. Lett. **111**, 158102 (2013).
- D. Shao, H. Levine, and W.-J. Rappel, Proc. Natl. Acad. Sci. U.S.A. **109**, 6851 (2012).
- D. Shao, W.-J. Rappel, and H. Levine. Phys. Rev. Lett. **105**, 108104 (2010).

For Further Reading III

- Toward a thermodynamically consistent picture of the phase-field model of vesicles: Curvature energy.
  D. Jamet, and C. Misbah, Phys. Rev. E **78**, 031902 (2008).
- Thermodynamically consistent picture of the phase-field model of vesicles: Elimination of the surface tension.
  D. Jamet, and C. Misbah, Phys. Rev. E **78**, 041903 (2008).
- Towards a thermodynamically consistent picture of the phase-field model of vesicles: Local membrane incompressibility.
  D. Jamet, and C. Misbah, Phys. Rev. E **76**, 051907 (2007).
- Phase-field approach to three-dimensional vesicle dynamics.
  T. Biben, K. Kassner, and C. Misbah, Phys. Rev. E **72**, 041921 (2005).